Neutral Color Semitransparent Microstructured Perovskite Solar Cells

Giles E. Eperon,[†] Victor M. Burlakov,[‡] Alain Goriely,[‡] and Henry J. Snaith[†,*]

[†]Department of Physics, University of Oxford, Clarendon Laboratory, Parks Road, Oxford OX1 3PU, United Kingdom and [‡]Mathematical Institute, OCCAM, University of Oxford, 24-29 St Giles, Oxford OX1 3LB, United Kingdom

ABSTRACT Neutral-colored semitransparent solar cells are commercially desired to integrate solar cells into the windows and cladding of buildings and automotive applications. Here, we report the use of morphological control of perovskite thin films to form semitransparent planar heterojunction solar cells with neutral color and comparatively high efficiencies. We take advantage of spontaneous dewetting to create microstructured arrays of perovskite "islands", on a length-scale small enough to appear continuous to the eye yet large enough to enable unattenuated transmission of light between the islands. The islands are thick enough to absorb most visible light, and the combination of completely absorbing and completely transparent regions results in neutral transmission of light. Using these films, we fabricate thin-film solar cells with respectable power conversion efficiencies. Remarkably, we find that such discontinuous films still have good rectification behavior and relatively high open-circuit voltages due to the inherent rectification between the n- and p-type charge collection layers. Furthermore, we demonstrate the ease of "color-tinting" such microstructured perovksite solar cells with no reduction in performance, by incorporation of a dye within the hole transport medium.

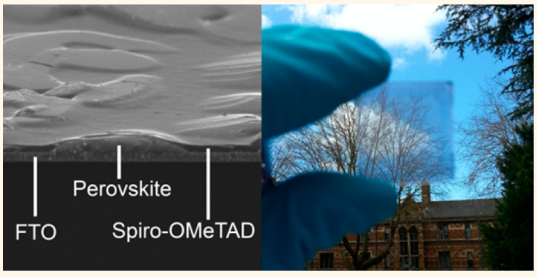

KEYWORDS: perovskite · solar cell · semitransparent · photovoltaics · building-integrated photovoltaics · neutral color · microstructured

Building-integrated photovoltaics (BIPV) are an attractive concept for economic generation of solar power.[1] Integration of semitransparent solar cells into windows is of particular interest since it opens the prospect of employing the entire façade of a building for solar power generation, rather than simply employing the limited roof space. In order for such solar glazing to be practical, costs must be low, and ideally they can be manufactured through existing coating methods employed in the glazing industry. They need to generate significant power while still having good transparency. Furthermore, while colored windows are interesting for novel applications, and a "splash" of color is desirable, the largest demand is for neutral-color tinted windows with controllable levels of transparency.

Some of the most successful approaches to achieve semitransparency in solar cells have used organic or dye-sensitized solar cells (OPVs and DSSCs, respectively).[2−7] These technologies are solution-processable, representing a low-cost production method and easy scalability.[8] Impressive recent progress has been made with neutral-colored OPVs.[7,9,10] However, their efficiencies are unlikely to reach those of crystalline technologies in the near future, due to large energy losses occurring at charge transfer interfaces.[11,12] To attain color-neutrality with organics, the active materials must be chosen carefully, often at a loss to overall efficiency.[3,4,13] An option with thin-film solar technologies, where the solar cell comprises a solid absorber layer, is to simply reduce the thickness of the absorber layer to allow transparency. Indeed, this is precisely what is done with amorphous silicon, currently being installed in BIPV applications. However, due to the precise nature of the density of states in the conduction and valence band in a crystalline semiconductor, the absorption coefficient increases monotonically from the band gap and thin films will assume a red or brown tint. Even though "bronze" is a choice for solar glazing, it does not represent the most desirable option.

Semiconducting perovskites have recently emerged as a new and intriguing class of photovoltaic materials. They have

* Address correspondence to h.snaith1@physics.ox.ac.uk.

Received for review October 7, 2013 and accepted December 3, 2013.

Published online 10.1021/nn4052309

properties similar to bulk inorganic semiconductors but can be processed at low temperatures using inexpensive and abundant materials.[14−20] They have now demonstrated surprisingly high power conversion efficiencies of over 15% in a range of device configurations.[21,22] Our recent work has shown that high-efficiency $CH_3NH_3PbI_{3-x}Cl_x$ perovskite solar cells can be produced at low temperatures and in a fully planar thin-film architecture, reducing fabrication steps and simplifying the design.[18,23] These characteristics make such perovskites ideal materials for fabrication of semitransparent windows. However, they fall firmly within the thin-film category, and a thin continuous perovskite film suffers from the same reddish-brown tint as conventional semiconductors.

We have recently investigated and developed a methodology to control the fractional surface coverage of $CH_3NH_3PbI_{3-x}Cl_x$ perovskite films, with the target of obtaining uniform and complete coating.[23] Perovskite films are deposited from spin-coating a precursor with a molar excess of organic and halide components and typically contain several small pores as-cast. Upon annealing, mass loss of the solvent and excess organic (CH_3NH_3) and halide (I or Cl) components allows morphological change due to minimization of surface energy.[23] The evolution of morphology depends upon several parameters. We found that by controlling parameters such as the initial film thickness, annealing temperature, atmosphere, and solvent vapor pressure, we could control whether pores in general opened or closed and, as such, achieved close to 100% surface coverage and highly efficient planar heterojunction solar cells.[23,24]

In addition to maximizing surface coverage, we can make use of incomplete surface coverage. Herein, we leverage dewetting of such films to form microstructured arrays of perovskite "islands". The perovskite islands are thick enough to absorb all visible light, whereas the "dewet" regions (absent of perovskite) are visibly transparent. As such, we form a semitransparent layer while avoiding the brown tint observed in thin semiconductor films; the overall optical appearance of such a film is neutral-colored. By varying the extent of dewetting, we control the transparency of the film, resulting in tunable and efficient semitransparent solar cells. This work now endows the perovskite technology with the neutral uniform coloration previously exclusive to organics.

RESULTS AND DISCUSSION

In Figure 1a, we show a schematic of the dewetting process to produce discontinuous regions of the perovskite absorber $CH_3NH_3PbI_{3-x}Cl_x$. Over time, pore growth, controllable through processing conditions such as temperature and film thickness, dictates the final morphology of the polycrystalline film. In Figure 1b, we show an SEM image of a representative semitransparent perovksite film formed to maximize open area. We measured the islands to be >1 μm in height. Visibly, such films appear neutral-colored (Figure 1c)—a 1 μm film of perovksite absorbs effectively all light at energies above its band gap, which is 1.55 eV.[20] A continuous 1 μm film would hence appear black, but because the perovskite film is formed of discontinuous islands, it appears semitransparent and of neutral color. For neutral color to be achieved, it is a prerequisite that the absorption onset of the absorber is in the near-infrared.

In order to characterize such films for their use in working solar cells, we are interested in the optical behavior of not just the perovskite but the whole active layer necessary to produce a working solar cell. Here, the device architecture is a planar heterojunction of perovskite between an n-type compact TiO_2 layer and a p-type hole transporter, 2,2′,7,7′-tetrakis-(*N*,*N*-di-*p*-methoxyphenylamine)-9,9′-spirobifluorene (spiro-OMeTAD). As such, from now, we define the "active layer" as the structure: compact TiO_2/perovskite/spiro-OMeTAD. Furthermore, as the application for semitransparent solar cells is for visible aesthetics, we are interested in the visible wavelengths, between 370 and 740 nm. We define the average visible transmittance (AVT) as the mean transmittance of a film between these wavelengths.

We fabricated perovskite films on compact TiO_2-coated FTO glass under a range of processing conditions (see Supporting Information) in order to achieve a wide range of transparencies. We measured the perovskite surface coverage *via* analysis of SEM images, then applied the spiro-OMeTAD layer and measured the AVT with an integrating sphere (details in Supporting Information). In Figure 1d, we show the dependence of AVT on perovskite surface coverage. A linear trend demonstrates the ease of controlling the transparency of such films by careful choice of solvent and processing temperature. We show a selection of representative active layer transmittance spectra in Figure 1e. We see encouragingly flat spectra across the majority of the visible spectrum, especially for the more transmissive samples. For the less transmissive samples (especially D and E in Figure 1e), there is a higher perovskite surface coverage, or less dewetting. These films were fabricated from the same solution concentrations and spin-coating protocol, but simply using different solvents, and dried and crystallized at different temperatures between 90 and 130 °C. For the same amount of starting material, the final film volume should be the same regardless of the extent of dewetting, hence the regions of perovskite in the films with more coverage are thinner and evidentially not thick enough to fully absorb the light at the red end of the spectrum. This is seen in Figure 1e, where even with 100% perovskite coverage, AVT is not 0%. The more dewet films comprise thicker perovskite islands and hence have flatter spectra. Diagrams of the cross

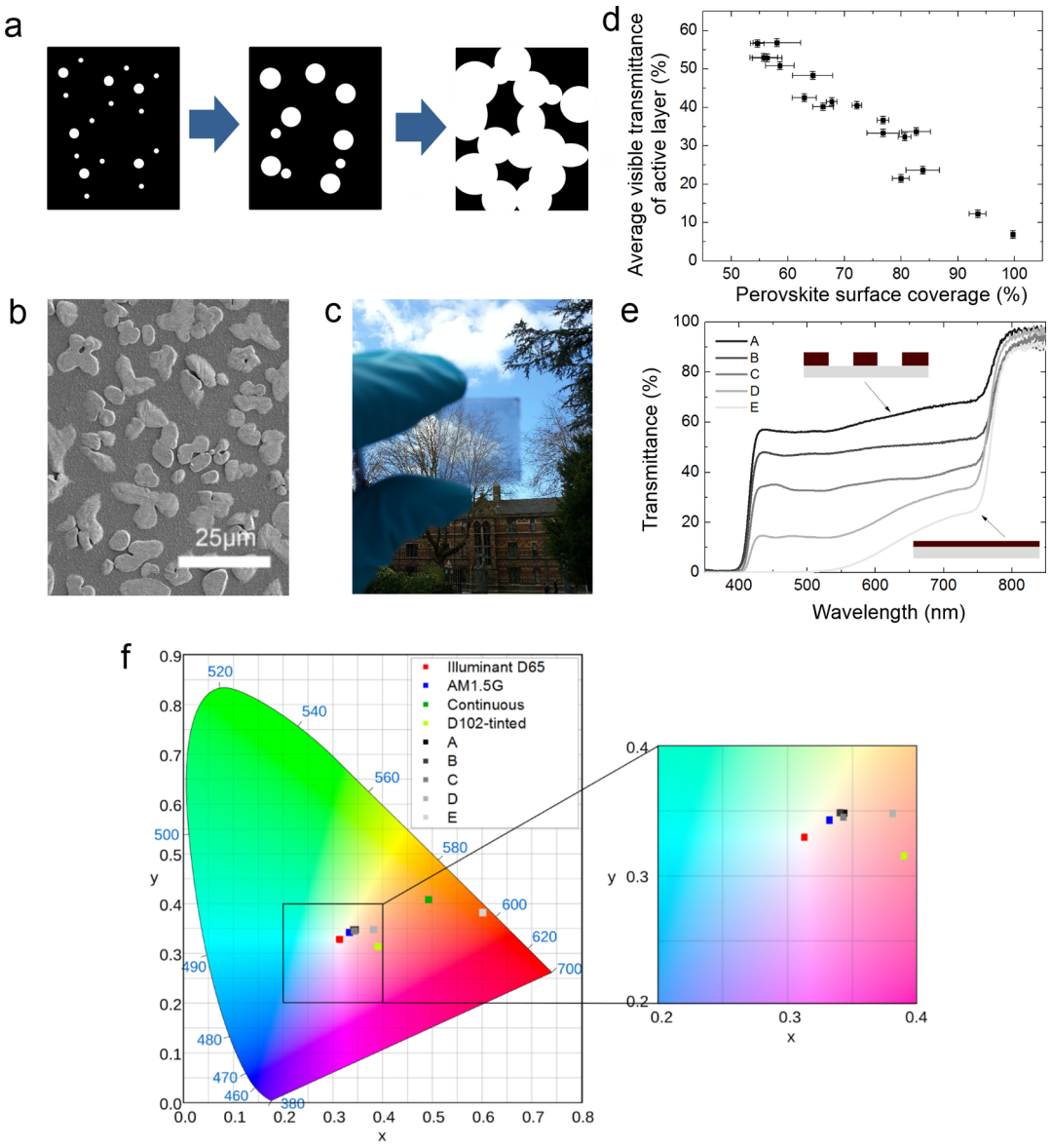

Figure 1. Controlled dewetting to vary transmittance of a perovskite film. (a) Schematic of the film dewetting process showing morphology change over time, from as-cast film to discrete islands. Perovskite material is represented with black and pores with white. (b) Scanning electron micrograph of the top surface of a representative film of perovskite islands (paler regions) on a TiO_2-coated FTO substrate. (c) Photograph through a typical semitransparent perovskite film formed on glass, demonstrating neutral color and semitransparency. (d) Dependence of average visible transmittance of the active layer on perovskite surface coverage. (e) Transmittance spectra of active layers of a selection of dewet perovskite devices. Diagrammatical representations of the most and least transparent films are shown as insets. (f) Color coordinates of the films with transmittance spectra shown in (d) under AM1.5 illumination, on the CIE *xy* 1931 chromacity diagram, and the enlarged central region. Color coordinates of a thin continuous perovskite film, a D102 dye-tinted cell (described later), the D65 standard daylight illuminant, and AM1.5 illumination are also shown.

section of high and low transmission films are shown as an inset to Figure 1e.

To quantify the color-neutrality of the active layers, we calculated color perception indices using the CIE 1931 *xy* color space, designed to represent human visual color perception. The transmitted light is represented by the product of the AM1.5 solar spectrum and the transmission spectrum of the active layer in question.[3,25] We calculated *x* and *y* color parameters for the samples labeled A–E in Figure 1e and display the results on the CIE 1931 *xy* chromacity diagram in Figure 1f. We also plot a ~200 nm thick continuous perovskite film, the reference daylight illuminant D65, and the AM1.5 spectrum. The color coordinates of the most transmissive active layers (A–C) are located very close to the AM1.5 spectrum and the D65 reference in the low colorfulness region of the chromacity diagram, representing excellent color-neutrality. At lower transmittances, films move toward the red-brown side of the chromacity diagram, where the thin continuous perovskite film is positioned.

We fabricated planar heterojunction solar cells with a range of transmittances, with the architecture shown

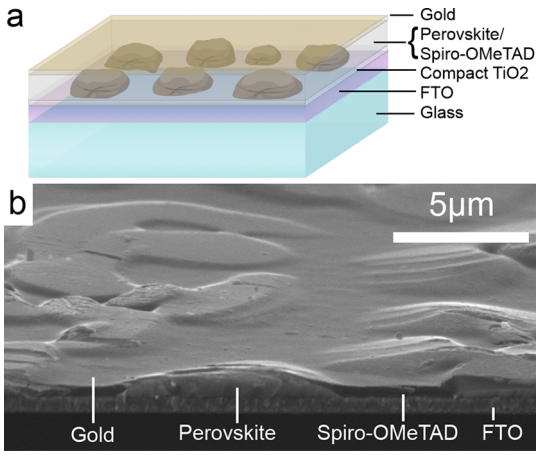

Figure 2. Semitransparent neutral-colored perovskite solar cells. (a) Diagram showing the architecture of the dewet planar perovskite heterojunction solar cell. (b) Tilted cross-sectional SEM image of a full semitransparent solar cell showing the perovskite islands coated with spiro-OMeTAD.

in Figure 2a. An SEM image of a cross section of a full device is shown in Figure 2b. The perovskite islands can be clearly seen, with the spiro-OMeTAD infiltrating the spaces between and also coating the islands with a thin layer. Ideally, we would use extremely transparent and conductive electrodes on both sides in order to maintain high transparencies. However, full optimization of the electrodes is beyond the scope of this study, and here we used fluorene-doped tin oxide (FTO) as the anode and a thin (~10 nm) layer of gold as the cathode. Such devices are reasonably transparent, though the gold electrode is a major source of transmittance loss (see Supporting Information Figure S3).

In Figure 3a, we plot the power conversion efficiencies against the AVT of the whole device (including 10 nm gold electrode) from a single batch of devices, extracted from current density–voltage curves measured under simulated AM1.5, 100 mW cm^{-2} sunlight. We observe a clear trend; at the lowest transmittances in this batch (AVT ~7%), power conversion efficiencies approach 8%, and as transmittance increases, the efficiency decreases. The most transparent cells, with AVTs of ~30%, showed power conversion efficiencies of around 3.5%. In Figure 3b, we show average current density–voltage curves from the same devices split into intervals of AVT. We observe a reduction in photocurrent for the higher transmittance devices. As expected, more light passes straight through the device. Remarkably, we find that device yield in these highly discontinuous films does not suffer from critical shunting, as might be expected based on other thin-film solar cells. Although there is a significant spread in device efficiency at similar transmittances, few devices were entirely nonfunctioning, and the lower coverage films did not show a greater spread. An interesting observation is that open-circuit voltage (V_{oc}) is similar at ~0.7 V for all but the least transmissive set of cells,

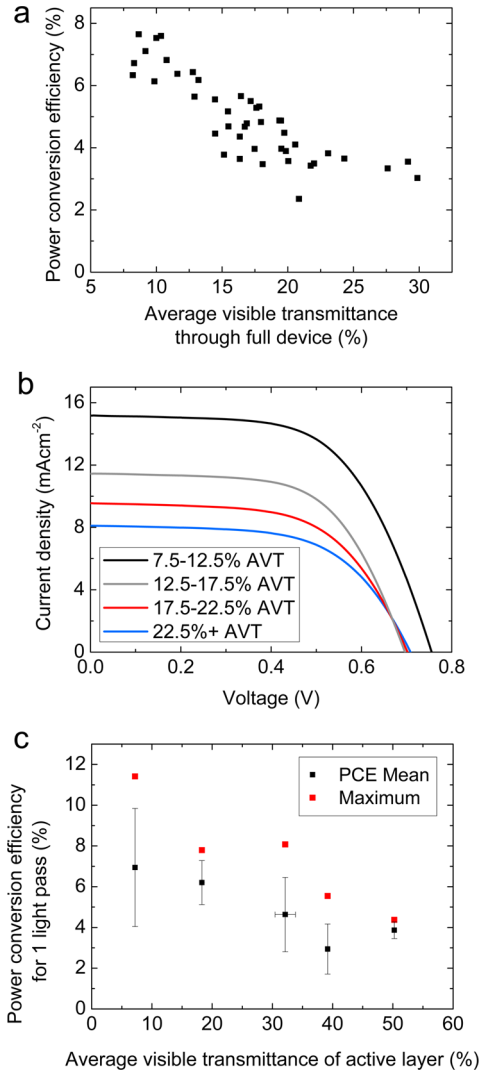

Figure 3. Semitransparent solar cell device performance. (a) Power conversion efficiencies for a batch of individual solar cells with ~10 nm Au electrodes, plotted as a function of full device AVT. (b) Average current density–voltage (J–V) characteristics for the cells plotted in (a). The curves are numerical averages of the current–voltage characteristics for individual cells split into the AVT intervals shown, with 5–15 cells per interval. (c) Power conversion efficiency plotted as a function of active layer AVT for a different batch of cells with thicker gold electrodes. The PCE plotted represents that which is attainable with an entirely transparent cathode (not a thick gold cathode). It has been corrected to remove current generated in the second pass (see Supporting Information for details on calculation). Each point represents the mean of at least 14 individual devices, and the maximum PCE for the champion device in each interval is plotted. In all cases, PCE was extracted from current–voltage measurements performed under 100 mW cm^{-2} AM1.5 illumination. Full performance data for all devices in this figure are shown in Supporting Information Tables ST1 and ST2.

where it is raised to ~0.75 V. We propose that greater perovskite coverage reduces spiro-OMeTAD/compact TiO_2 contact area, and these regions represent a parallel diode to the photoactive regions, with a lower shunt resistance. Hence, increasing the perovskite coverage increases the overall shunt resistance and increases the V_{oc}. From these J–V curves, it appears

that, for the higher transmittances (*i.e.*, lower perovskite coverage), the V_{oc} reaches a minimum of ~0.7 V. To further understand this, we fabricated and tested spiro-OMeTAD/compact TiO_2 diodes. Their diode characteristics show a dark current turn-on at also ~0.7 V (see Supporting Information), so even in the case of there being minimum perovskite coverage, we would not expect the diode turn-on voltage to be any lower than 0.7 V, and hence this sets a lower limit on the open-circuit voltage. With full perovskite coverage, spiro-OMeTAD/perovskite/compact TiO_2 devices have been observed to have an open-circuit voltage of >1 V.[22] Thus, with higher perovskite coverage, the fraction of spiro-OMeTAD/perovskite/compact TiO_2 diode area compared to spiro-OMeTAD/compact TiO_2 will increase, and the effective turn-on voltage of these parallel diodes should increase from 0.7 to >1 V, as seen.

The electrodes used (FTO and 10 nm thick gold) are non-optimum transparent electrodes. Much work is being undertaken to develop highly transmissive and conductive electrodes for semitransparent solar cells and other applications.[26] In light of this, we determined the best performance that could be achieved from these solar cells if we could use an entirely transparent cathode. We fabricated devices with a number of different active layer AVTs, between 5 and 50%, and deposited slightly thicker gold electrodes to minimize electrode resistance. We determined the power conversion efficiency from measuring current–voltage characteristics and then corrected the photocurrent to remove the fraction of current generated by the second pass of reflected light from the gold electrode (see Supporting Information for details of calculation). We thus determined the PCE that could be attained from devices with entirely transparent cathodes (Figure 3c). We note that we have not increased the measured photocurrent to account for light absorbed in the FTO, and all the "corrected" photocurrents are lower than the measured photocurrents (Supporting Information Table ST2). Even so, we can see that significantly improved performance could be achieved in comparison to the devices employing the thin gold electrodes, at a given active layer AVT. Notably, ~30% AVT active layers would still generate power conversion efficiencies of over 8%, which is a transparency and a performance that is compatible with commercial applications, being better than currently offered by a-Si, and would represent the best semitransparent neutral-colored solar cell efficiency to date. Once we have resolved the lower open-circuit voltages in these microstructured perovskite solar cells, the V_{oc} should be able to be pushed up toward 1.1 V, which is achievable in uniform planar heterojunction solar cells,[22] which will result in another 20–30% increase in relative efficiency. In addition, we are still employing TEC7 FTO-coated glass, which is not the most transmissive conducting layer, and further improvements

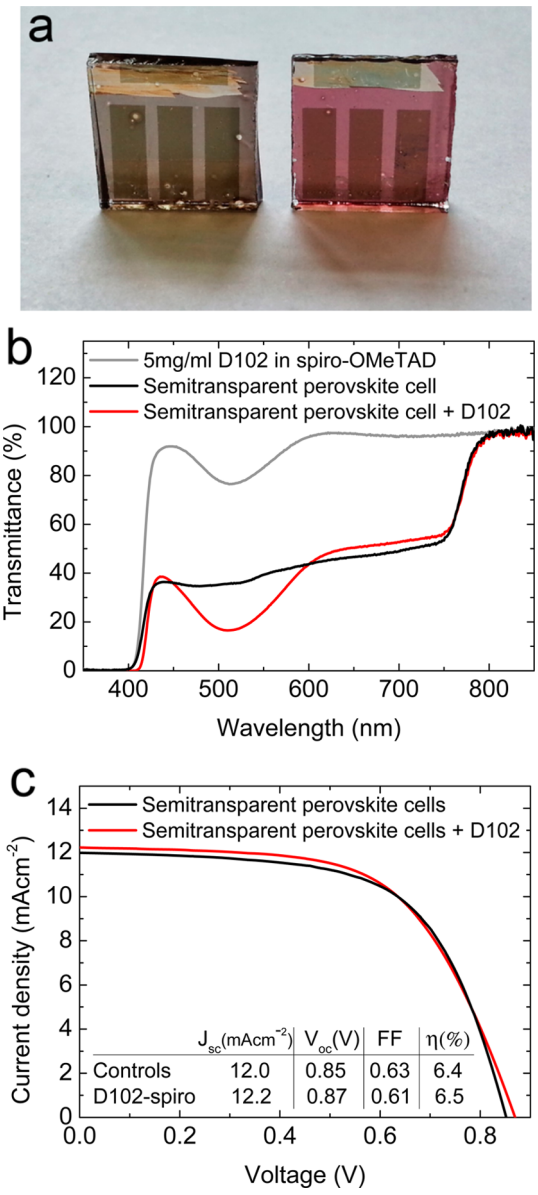

Figure 4. Color-tinted semitransparent solar cells. (a) Photographs of semitransparent perovskite solar cells without (left) and with (right) D102 dye included in the spiro-OMeTAD layer, with 10 nm gold electrodes. (b) Transmittance spectra of the active layer of such cells. (c) Average current density–voltage characteristics of such solar cells, demonstrating effectively no change in performance with inclusion of the dye. Device performance parameters are shown in the inset. Averages are numerical averages from nine D102-doped and 12 control cells.

are still possible by simply employing a more transparent anode and an anti-reflective coating (an estimation of the further increases in efficiency possible is discussed in the Supporting Information).

Having demonstrated a new and versatile means to form neutral-colored semitransparent solar cells, of further interest would be the prospect for lightly color-tinting such cells. With the microstructured architecture, we can envisage that it should be easy to optically modify the semitransparent cells by incorporation of a

dye or pigment into the regions where light passes through. Here, we simply dissolved an indolene dye termed D102 into the spiro-OMeTAD solution, and upon application to typical semitransparent cells, it produces "rose-tinted" devices (Figure 4a).[27] Plotting this tinted active layer on the chromacity diagram in Figure 1f shows that these films lie in the pale pink region. As we show in Figure 4b, the absorption peak of the dye in addition to the perovskite attenuation is apparent in the transmittance spectrum. While light absorbed by the dye will not contribute to photocurrent, device performance should remain unaltered provided the dye has not introduced any detrimental electronic artifacts. We show the current−voltage curves of such devices in Figure 4c which confirm this; on average, the rose-tinted cells perform similarly to the control cells.

Another way of providing semitransparency would be to use a wider band gap perovskite, of which there are many known examples.[19,28,29] However, this system would be restricted to the range of colors attainable with such a semiconductor (yellow, through red, to brown); the advantage of dye-tinting a neutral-colored "base" is that any color of dye or pigment could be incorporated, and those with proven resilience to long-term exposure to light, and even colors typically challenging to achieve with semiconductors such as green or blue.

There is no "ideal" semitransparent solar cell because it depends upon the color desired. For an application requiring colors achievable with a semiconductor, a continuous layer of wider band gap perovksite might be preferable. However, the novelty of the present work is that we have fabricated neutral-colored semitransparent solar cells. For color-neutrality, a band gap of ~1.6 eV or lower is necessary, so that a thick layer absorbs all visible light and hence looks black. This configuration also allows the addition of *any* color to the gray base, providing much greater flexibility in terms of independence of color and semitransparency.

As discussed briefly earlier, more transparent electrodes are necessary, specifically the cathode, for fully optimized semitransparent perovskite solar cells. For this purpose, low-temperature processable and ideally solution-processable electrodes need to be developed, which have toward 90% AVT with the order of 10 Ω/□ sheet resistivity and exhibit good ohmic contact to the hole transporter. Solutions may come from transparent conducting oxides, carbon nanotubes, graphene, or metallic nanowires, such as silver.[6,26,30−35]

A key concern for an application such as architectural glass is that of long-term stability. Power-generating glass must have a long functional lifetime to avoid the expense of replacing it regularly. The methylammonium lead halide perovskite is hygroscopic, indicating that substantive sealing from the atmosphere is required, facilitated by sealing between two glass sheets. Recent preliminary work on stability has also shown that, even with rudimentary sealing from the atmosphere, such solar cells are already relatively robust to prolonged exposure and operation under full spectrum sun light.[21,36] Ensuring the materials and solar cell composites are capable of attaining operational lifetimes of over 25 years should attract significant research attention going forward and is likely to be a surmountable challenge.

CONCLUSIONS

In summary, we have demonstrated the fabrication of neutral-colored semitransparent solar cells by creating microporous layers of organometal halide perovskite by partial dewetting of solution-cast films. Our complete devices show good efficiencies at reasonable levels of transparencies, with significant scope for further improvement by implementing electrodes with higher transparencies and enhancing the open-circuit voltage. Furthermore, we have demonstrated that the microstructured perovskite film concept can be easily adapted to integrate color into semitransparent devices with no loss in efficiency. This work now enables perovskite solar cells to not only compete for high-efficiency opaque applications but also offer an ideal solution to building integrated photovoltaics: neutral-color semitransparency at comparatively high efficiency.

METHODS

Materials. Unless otherwise stated, all materials were purchased from Sigma-Aldrich or Alfa Aesar and used as received. Spiro-OMeTAD was purchased from Borun Chemicals. CH_3NH_3I was synthesized in-house according to a reported procedure.[20]

Semitransparent Perovskite Solar Cell Preparation. Devices were fabricated on fluorine-doped tin oxide (FTO)-coated glass (Pilkington, 7 Ω/□). Initially, FTO was removed from regions under the anode contact by etching the FTO with 2 M HCl and zinc powder. Substrates were then cleaned sequentially in hallmanex detergent, acetone, propan-2-ol, and oxygen plasma. A ~50 nm hole-blocking layer of compact TiO_2 was deposited by spin-coating a mildly acidic solution of titanium isopropoxide in ethanol (350 μL in 5 mL of ethanol with 0.013 M HCl) at 2000 rpm and annealed at 500 °C for 30 min.

The dewet perovskite layers were deposited by spin-coating a nonstoichiometric precursor solution of methylammonium iodide and lead chlorine (3:1 molar ratio, final concentrations 0.88 M lead chloride and 2.64 M methylammonium iodide) in either dimethylsulfoxide (DMSO), *N*-methyl-2-pyrrolidone (NMP), or *N*,*N*-dimethylformamide (DMF) (not mixtures of). The films were then annealed to dewet and crystallize the perovskite. Details of the conditions used to produce a certain active layer transmittance are reported in the Supporting Information. Spin-coating and annealing were carried out in either air or a moisture- and oxygen-free glovebox (H_2O < 1 ppm) at 2000 rpm Annealing was carried out at a range of temperatures between 90 and 130 °C.

The hole-transporting layer was then deposited *via* spin-coating a 0.788 M solution in chlorobenzene of 2,2′,7,7′-tetrakis-(*N*,*N*-di-*p*-methoxyphenylamine)-9,9′-spirobifluorene

(spiro-OMeTAD), with additives of 0.0184 lithium bis(trifluoromethanesulfonyl)imide (added in 0.61 M acetonitrile solution) and 0.0659 M 4-*tert*-butylpyridine. Spin-coating was carried out in air at 2000 rpm.

Gold electrodes were thermally evaporated under vacuum of $\sim 10^{-6}$ Torr at a rate of ~0.1 nm/s to complete the devices. For semitransparent contacts, ~10 nm was deposited.

Device Characterization. The current density−voltage (*J*−*V*) curves were measured (2400 series sourcemeter, Keithley Instruments) under simulated AM1.5 sunlight at 100 mW cm^{-2} irradiance generated by an Abet Class AAB sun 2000 simulator, with the intensity calibrated with an NREL calibrated KG5 filtered Si reference cell. The mismatch factor was calculated to be less than 1%. The solar cells were masked with a metal aperture to define the active area, typically 0.09 cm^{-2} (measured individually for each mask), and measured in a light-tight sample holder to minimize any edge effects and ensure that the reference cell and test cell are located during measurement in the same spot under the solar simulator.

Optical Measurements. Transmittance and reflectance spectra were collected with a Varian Cary 300 UV−vis spectrophotometer with an internally coupled integrating sphere.

Film Characterization. A Hitachi S-4300 field emission scanning electron microscope and a FEI Inspect S50 tungsten source scanning electron microscope were used to acquire SEM images. To determine coverage of perovskite films from SEM images, ImageJ[37] was used to define a grayscale threshold such that the perovskite was distinct from the substrate, and percentage coverage was then calculated by the program. Sample thicknesses were measured using a Veeco Dektak 150 surface profilometer.

Conflict of Interest: The authors declare no competing financial interest.

Acknowledgment. This work was supported by EPSRC and Oxford Photovoltaics Ltd. through a Nanotechnology KTN CASE award, the European Research Council (ERC) HYPER PROJECT No. 279881. This publication is based in part upon work supported by Award No. KUK-C1-013-04, made by King Abdullah University of Science and Technology (KAUST). A.G. is a Wolfson/Royal Society Merit Award Holder and acknowledges support from a Reintegration Grant under EC Framework VII. V.B. is an Oxford Martin School Fellow, and this work was in part supported by the Oxford Martin School. The authors wish to thank Maximillian Hoerantner for assistance in graphical design.

Supporting Information Available: Detailed description of dewetting control, calculations of active layer transmittance, transmissive losses due to gold electrode, correction to remove second pass of light reflected from electrodes, estimation of extra photocurrent available with a fully transparent anode, and current−voltage characteristics for a diode with no perovksite layer. This material is available free of charge *via* the Internet at http://pubs.acs.org.

REFERENCES AND NOTES

1. Henemann, A. BIPV: Built-in Solar Energy. *Renewable Energy Focus* **2008**, *9*, 14–19.
2. Kang, M. G.; Park, N.-G.; Park, Y. J.; Ryu, K. S.; Chang, S. H. Manufacturing Method for Transparent Electric Windows Using Dye-Sensitized TiO_2 Solar Cells. *Sol. Energy Mater. Sol. Cells* **2003**, *75*, 475–479.
3. Chen, K.-S.; Salinas, J.-F.; Yip, H.-L.; Huo, L.; Hou, J.; Jen, A. K.-Y. Semi-transparent Polymer Solar Cells with 6% PCE, 25% Average Visible Transmittance and a Color Rendering Index Close to 100 for Power Generating Window Applications. *Energy Environ. Sci.* **2012**, *5*, 9551–9557.
4. Chiang, Y.-F.; Chen, R.-T.; Burke, A.; Bach, U.; Chen, P.; Guo, T.-F. Non-color Distortion for Visible Light Transmitted Tandem Solid State Dye-Sensitized Solar Cells. *Renewable Energy* **2013**, *59*, 136–140.
5. Chueh, C.-C.; Chien, S.-C.; Yip, H.-L.; Salinas, J. F.; Li, C.-Z.; Chen, K.-S.; Chen, F.-C.; Chen, W.-C.; Jen, A. K.-Y. Toward High-Performance Semi-transparent Polymer Solar Cells: Optimization of Ultra-thin Light Absorbing Layer and Transparent Cathode Architecture. *Adv. Energy Mater.* **2013**, *3*, 417–423.
6. Chen, C.; Dou, L.; Zhu, R.; Chung, C.; Song, T.; Zheng, Y. B.; Hawks, S.; Li, G.; Weiss, P. S.; Yang, Y. Visibly Transparent Polymer Solar Cells Produced by Solution Processing. *ACS Nano* **2012**, *6*, 7185–7190.
7. Bailey-Salzman, R. F.; Rand, B. P.; Forrest, S. R. Semitransparent Organic Photovoltaic Cells. *Appl. Phys. Lett.* **2006**, *88*, 233502.
8. Krebs, F. C.; Tromholt, T.; Jørgensen, M. Upscaling of Polymer Solar Cell Fabrication Using Full Roll-to-Roll Processing. *Nanoscale* **2010**, *2*, 873–886.
9. Colsmann, A.; Puetz, A.; Bauer, A.; Hanisch, J.; Ahlswede, E.; Lemmer, U. Efficient Semi-transparent Organic Solar Cells with Good Transparency Color Perception and Rendering Properties. *Adv. Energy Mater.* **2011**, *1*, 599–603.
10. Chen, C.-C.; Dou, L.; Gao, J.; Chang, W.-H.; Li, G.; Yang, Y. High-Performance Semi-transparent Polymer Solar Cells Possessing Tandem Structures. *Energy Environ. Sci.* **2013**, *6*, 2714–2720.
11. Snaith, H. J. Estimating the Maximum Attainable Efficiency in Dye-Sensitized Solar Cells. *Adv. Funct. Mater.* **2010**, *20*, 13–19.
12. Kirchartz, T.; Taretto, K.; Rau, U. Efficiency Limits of Organic Bulk Heterojunction Solar Cells. *J. Phys. Chem. C* **2009**, *113*, 17958–17966.
13. Ameri, T.; Dennler, G.; Waldauf, C.; Azimi, H.; Seemann, A.; Forberich, K.; Hauch, J.; Scharber, M.; Hingerl, K.; Brabec, C. J. Fabrication, Optical Modeling, and Color Characterization of Semitransparent Bulk-Heterojunction Organic Solar Cells in an Inverted Structure. *Adv. Funct. Mater.* **2010**, *20*, 1592–1598.
14. Kim, H.-S.; Lee, C.-R.; Im, J.-H.; Lee, K.-B.; Moehl, T.; Marchioro, A.; Moon, S.-J.; Humphry-Baker, R.; Yum, J.-H.; Moser, J. E.; *et al.* Lead Iodide Perovskite Sensitized All-Solid-State Submicron Thin Film Mesoscopic Solar Cell with Efficiency Exceeding 9%. *Sci. Rep.* **2012**, *2*, 591.
15. Im, J.-H.; Lee, C.-R.; Lee, J.-W.; Park, S.-W.; Park, N.-G. 6.5% Efficient Perovskite Quantum-Dot-Sensitized Solar Cell. *Nanoscale* **2011**, *3*, 4088–4093.
16. Kojima, A.; Teshima, K.; Shirai, Y.; Miyasaka, T. Organometal Halide Perovskites as Visible-Light Sensitizers for Photovoltaic Cells. *J. Am. Chem. Soc.* **2009**, *131*, 6050–6051.
17. Chung, I.; Lee, B.; He, J.; Chang, R. P. H.; Kanatzidis, M. G. All-Solid-State Dye-Sensitized Solar Cells with High Efficiency. *Nature* **2012**, *485*, 486–489.
18. Ball, J. M.; Lee, M. M.; Hey, A.; Snaith, H. J. Low-Temperature Processed Mesosuperstructured to Thin-Film Perovskite Solar Cells. *Energy Environ. Sci.* **2013**, *6*, 1739–1743.
19. Noh, J. H.; Im, S. H.; Heo, J. H.; Mandal, T. N.; Seok, S. I. Chemical Management for Colorful, Efficient, and Stable Inorganic−Organic Hybrid Nanostructured Solar Cells. *Nano Lett.* **2013**, *13*, 1764–1769.
20. Lee, M. M.; Teuscher, J.; Miyasaka, T.; Murakami, T. N.; Snaith, H. J. Efficient Hybrid Solar Cells Based on Meso-superstructured Organometal Halide Perovskites. *Science* **2012**, *338*, 643–647.
21. Burschka, J.; Pellet, N.; Moon, S.-J.; Humphry-Baker, R.; Gao, P.; Nazeeruddin, M. K.; Grätzel, M. Sequential Deposition as a Route to High-Performance Perovskite-Sensitized Solar Cells. *Nature* **2013**, *499*, 316–319.
22. Liu, M.; Johnston, M. B.; Snaith, H. J. Efficient Planar Heterojunction Perovskite Solar Cells by Vapour Deposition. *Nature* **2013**, *501*, 395–398.
23. Eperon, G. E.; Burlakov, V. M.; Docampo, P.; Goriely, A.; Snaith, H. J. Morphological Control for High Performance, Solution-Processed Planar Heterojunction Perovskite Solar Cells. *Adv. Funct. Mater.* **2013**, 10.1002/adfm.201302090.
24. Stranks, S. D.; Eperon, G. E.; Grancini, G.; Menelaou, C.; Alcocer, M. J. P.; Leijtens, T.; Herz, L. M.; Petrozza, A.; Snaith, H. J. Electron−Hole Diffusion Lengths Exceeding 1 Micron in an Organometal Trihalide Perovskite Absorber. *Science* **2013**, *342*, 341–344.
25. Smith, T.; Guild, J. The CIE Colorimetric Standards and Their Use. *Trans. Opt. Soc.* **1932**, *33*, 73–134.

26. Ellmer, K. Past Achievements and Future Challenges in the Development of Optically Transparent Electrodes. *Nat. Photonics* **2012**, *6*, 809–817.
27. Schmidt-Mende, L.; Bach, U.; Humphry-Baker, R.; Horiuchi, T.; Miura, H.; Ito, S.; Uchida, S.; Grätzel, M. Organic Dye for Highly Efficient Solid-State Dye-Sensitized Solar Cells. *Adv. Mater.* **2005**, *17*, 813–815.
28. Im, J.-H.; Chung, J.; Kim, S.-J.; Park, N.-G. Synthesis, Structure, and Photovoltaic Property of a Nanocrystalline 2H Perovskite-Type Novel Sensitizer $CH_3CH_2NH_3PbI_3$. *Nanoscale Res. Lett.* **2012**, *7*, 353.
29. Mitzi, D. B. In *Progress in Inorganic Chemistry*; Karlin, K. D., Ed.; John Wiley & Sons: New York, 1999; Vol. 48, pp 1−122.
30. Gaynor, W.; Burkhard, G. F.; McGehee, M. D.; Peumans, P. Smooth Nanowire/Polymer Composite Transparent Electrodes. *Adv. Mater.* **2011**, *23*, 2905–2910.
31. Krantz, J.; Stubhan, T.; Richter, M.; Spallek, S.; Litzov, I.; Matt, G. J.; Spiecker, E.; Brabec, C. J. Spray-Coated Silver Nanowires as Top Electrode Layer in Semitransparent P3HT:PCBM-Based Organic Solar Cell Devices. *Adv. Funct. Mater.* **2012**, *23*, 1711–1717.
32. Yang, D.; Meng, G.; Zhang, S.; Hao, Y.; An, X.; Wei, Q.; Ye, M.; Zhang, L. Electrochemical Synthesis of Metal and Semimetal Nanotube−Nanowire Heterojunctions and Their Electronic Transport Properties. *Chem. Commun.* **2007**, *1*, 1733–1735.
33. Wu, J.; Becerril, H. A.; Bao, Z.; Liu, Z.; Chen, Y.; Peumans, P. Organic Solar Cells with Solution-Processed Graphene Transparent Electrodes. *Appl. Phys. Lett.* **2008**, *92*, 263302.
34. Wang, X.; Zhi, L.; Müllen, K. Transparent, Conductive Graphene Electrodes for Dye-Sensitized Solar Cells. *Nano Lett.* **2008**, *8*, 323–327.
35. van de Lagemaat, J.; Barnes, T. M.; Rumbles, G.; Shaheen, S. E.; Coutts, T. J.; Weeks, C.; Levitsky, I.; Peltola, J.; Glatkowski, P. Organic Solar Cells with Carbon Nanotubes Replacing In_2O_3:Sn as the Transparent Electrode. *Appl. Phys. Lett.* **2006**, *88*, 233503.
36. Leijtens, T.; Eperon, G. E.; Pathak, S.; Abate, A.; Lee, M. M.; Snaith, H. J. Overcoming Ultraviolet Light Instability of Sensitized TiO_2 with Meso-superstructured Organometal Trihalide Perovskite Solar Cells. *Nat. Commun.* **2013**, 10.1038/ncomms3885.
37. Rasband, W. *ImageJ* 2005, http://rsb.info.nih.gov/ij/.